Fields Institute Communications
Volume **00**, 0000

A Note on the Dynamics of Piecewise-Autonomous Bistable Parabolic Equations

Bernold Fiedler
Freie Universität Berlin
Institut für Mathematik I
Arnimallee 2–6
D – 14195 Berlin
Germany
fiedler@math.fu-berlin.de

Carlos Rocha
Departamento de Matemática
Instituto Superior Técnico
Av. Rovisco Pais
1049–001 Lisbon
Portugal
crocha@math.ist.utl.pt

Domingo Salazar
University of Oxford
Mathematical Institute
24–29 St. Giles'
Oxford
OX1 3LB
United Kingdom
salazar@maths.ox.ac.uk

Joan Solà-Morales
Departament de Matemàtica Aplicada 1
Universitat Politècnica de Catalunya
Av. Diagonal, 647
08028–Barcelona
Spain
jsola@ma1.upc.es

Dedicated to Professor Waldyr M. Oliva on his 70th birthday.

2000 *Mathematics Subject Classification.* Primary 35K20, 37C70.

Key words and phrases. reaction-diffusion equations, Morse index, global attractor, meander permutation.

B. Fiedler is partially supported by the Deutsche Forschungsgemeinschaft. C. Rocha is partially supported by FCT (Portugal) through the Research Units Pluriannual Funding Program. D. Salazar is supported by TMR ERBFMRXCT 97–0117, EU. J. Solà-Morales is partially supported by project PB98-0932-C02-01 of CICYT, Spain.

Abstract. For a family of piecewise-autonomous one-dimensional bistable parabolic equations, with vanishing diffusion and Neumann boundary conditions, we determine the number and Morse indices of their equilibria as a function of the number of subintervals where the equations are autonomous. We conjecture how to build their attractors in a recursive way as the number of subintervals increases.

1 Introduction

Given an integer $k > 1$ and a partition of the interval $(0, 1)$ into k pieces of the form (x_{i-1}, x_i) with $0 = x_0 < x_1 < x_2 < \cdots < x_k = 1$ we are going to consider the evolution problem defined by the following reaction-diffusion equation with a piecewise x-independent reaction:

$$\begin{cases} u_t = \epsilon^2 u_{xx} + u(1-u)(u - c(x)), & 0 < x < 1; \\ u_x(0) = u_x(1) = 0, & \\ c(x) = c_i, & \text{for } x \in (x_{i-1}, x_i),\ c_i \in (0,1). \end{cases} \tag{1.1}$$

This type of nonlinearity has received some attention, mainly in the case of a smooth function $c(x)$ (see [1], [4], and [12]), but also in the piecewise constant case (see [16]).

In a recent work [17], it was shown that, for small ϵ, the asymptotic behaviour of the solutions of (1.1) as $t \to \infty$ turns out to be very different depending on whether all jumps of adjacent c_i are either small or large . In the first case, resembling the case when $c(x)$ is smooth, the global attractor becomes more and more complicated when $\epsilon \to 0$, in the sense that both the number of equilibrium solutions and their maximal Morse indices (and so, the topological dimension of the attractor) tend to infinity.

However, when the sequence $c_1, c_2, c_3 \ldots, c_k$ is near the sequence $0, 1, 0, 1, \ldots$ or $1, 0, 1, 0 \ldots$, the global attractor stabilises itself when $\epsilon \to 0$ and the number of equilibria, N_k, only depends on k. Specifically, N_k is given by the two-term recurrence $N_1 = 3$, $N_2 = 5$ and $N_{i+1} = N_i + 2N_{i-1}$, and explicitly by the formula $N_k = (2^{k+2} - (-1)^k)/3$. And the maximal Morse index of these equilibria is bounded by $2k$.

In June 2000, the results of [17] were presented in a communication to the Conference on Differential Equations and Dynamical Systems in honour of Prof. Waldyr Oliva. Questions and comments by the audience originated several joint work sessions and mail contacts among the present four authors. This note is a summary of the results obtained from this discussions.

The contents of this Note are the following: In Section 2, a pertinent part of the results of [17] is presented, together with the part of the proof that provides the main ideas and tools used subsequently. Section 3 presents a proof of a recurrence formula for the number of equilibria of a given Morse index as a function of k. In particular, the bound $\dim \mathcal{A}_k \leq 2k$ of [17] on the maximal Morse index is improved to $\dim \mathcal{A}_k = [(k+1)/2]$. Section 4 is devoted to the description of the global attractor $\mathcal{A}_k$, giving an algorithm to generate a meander permutation that characterises it, in the sense of [7], and obtaining geometrical descriptions of the lower-dimensional cases. A conjecture on a recursive geometric description of $\mathcal{A}_k$, for all k, is also presented.

2 Number of equilibria

The following statement partially reproduces Theorem 3 of [17]. In this section we present the geometric concepts behind the proof. For the complete proof, see [17].

Theorem 2.1 *Let $k > 1$ be an integer and $0 = x_0 < x_1 < \cdots < x_k = 1$. Let $c_1, c_2, \ldots, c_k$ be a sequence with $0 < c_i < 1$, for all i, and close enough to the sequence $0, 1, 0, 1, \ldots$ (the case close to $1, 0, 1, 0, \ldots$ reduces to the previous one by replacing u by $1 - u$).*

Then, if ϵ is small enough, the problem (1.1) possesses exactly N_k equilibrium solutions, where $N_{i+1} = N_i + 2N_{i-1}$ with initial values $N_0 = 1$, $N_1 = 3$. So one has $N_k = (2^{k+2} - (-1)^k)/3$ for $k \geq 2$, that is $N_i = 3, 5, 11, 21, 43, \ldots$

Proof To deal with the equation of equilibria, we work with the stretched variable x/ϵ that we rename x again. So, we have to find the solutions of

$$\begin{cases} u_{xx} + u(1-u)(u - c(x)) = 0, \\ u_x(0) = u_x(1/\epsilon) = 0, \\ c(x) = c_i, \qquad\qquad \text{for } x \in (x_{i-1}/\epsilon, x_i/\epsilon). \end{cases} \tag{2.1}$$

For a given i, the phase portraits of the differential equation

$$\ddot{u}(x) = -u(1-u)(u - c_i) \tag{2.2}$$

in the phase plane $(u, \dot{u})$ are easy to obtain and are depicted in Figure 1.

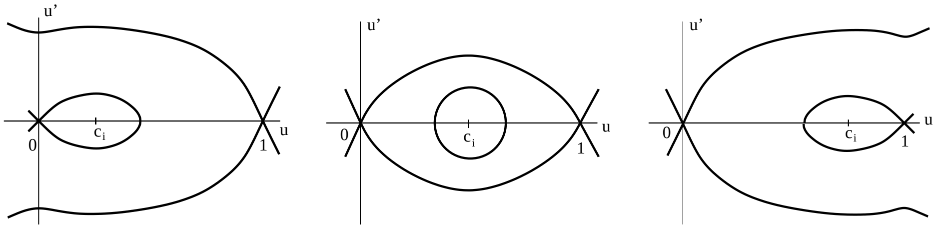

(a) $c_i < 1/2$ (b) $c_i = 1/2$ (c) $c_i > 1/2$

Figure 1 Phase portraits of (2.2) for different values of c_i.

The proof of Theorem 1 follows the evolution of the so-called *(forward) time map* or *shooting curve* L_y for $0 \leq y \leq 1/\epsilon$. The curves L_y in the $(u, \dot{u})$ plane, parametrised by $u_0 \in [0, 1]$, are defined as

$$L_y = \{(u(y), \dot{u}(y)), 0 \leq u_0 \leq 1\} \tag{2.3}$$

where $u(x)$ is the solution of 2.1 with initial values $(u(0), \dot{u}(0)) = (u_0, 0)$. It is clear that the equilibrium solutions are represented by the intersections of $L_{1/\epsilon}$ with the axis $\dot{u} = 0$. The proof follows the evolution of the time maps after each jump in $c(x)$, that is the evolution of the curves $L_{x_1/\epsilon}, L_{x_2/\epsilon}, \ldots, L_{x_k/\epsilon}$. In fact, one can show that only the intersections of these curves with the strip $0 \leq u \leq 1$ are of interest.

The following figures 2 and 3 show the evolution of the time map along the intervals $0 \le y \le x_1/\epsilon$ and $x_1/\epsilon \le y \le x_2/\epsilon$, when ϵ is small enough. Figure 3, also shows the existence of 5 equilibrium solutions when $k = 2$.

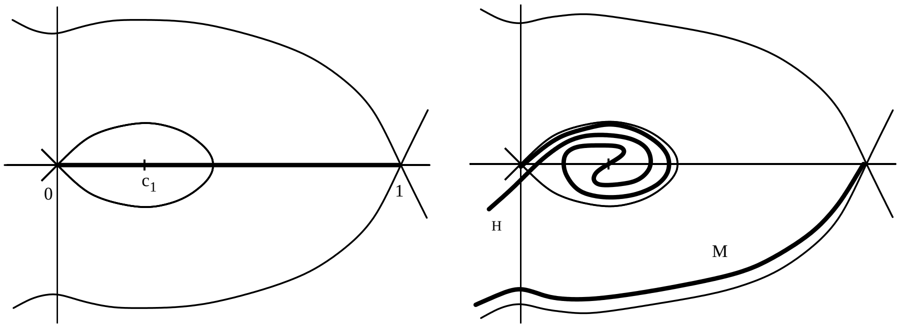

(a) Beginning (b) End

Figure 2 Evolution of L_y in the first interval

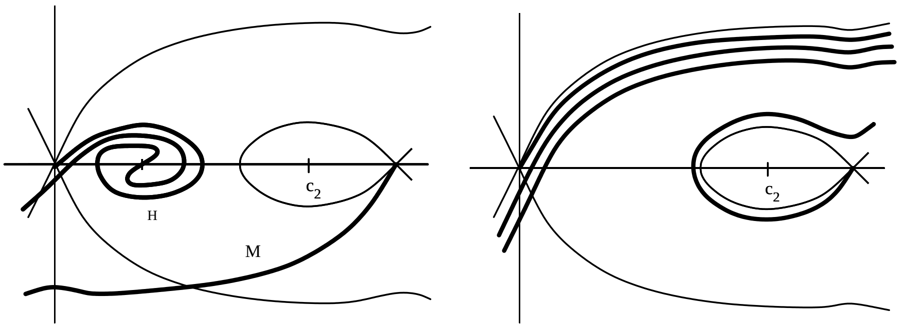

(a) Beginning (b) End

Figure 3 Evolution of L_y in the second interval

The proof in [17] made heavy use of the so-called λ-Lemma, which states that the shooting manifolds are going to get close in the C^1 topology to the unstable manifolds of the critical points as ϵ goes to zero (see [15]). Even so, special care must be taken in applying this result in order to get a correct count of the critical points because it is conceivable that something like what appears in figure 4 could happen along the second interval, showing the appearance of "fingers", whose number could increase when $\epsilon \to 0$. The hypotheses that c_1 is near 0 and c_2 is near 1 avoids that possibility (see [17] for details).

At the end of the second interval (see figure 3, (b)), the time map is made of three "manifolds", that approach in the C^1 sense one of the unstable manifolds of the equilibrium point $(0, 0)$, and one "hook", that follows, from outside, the orbit

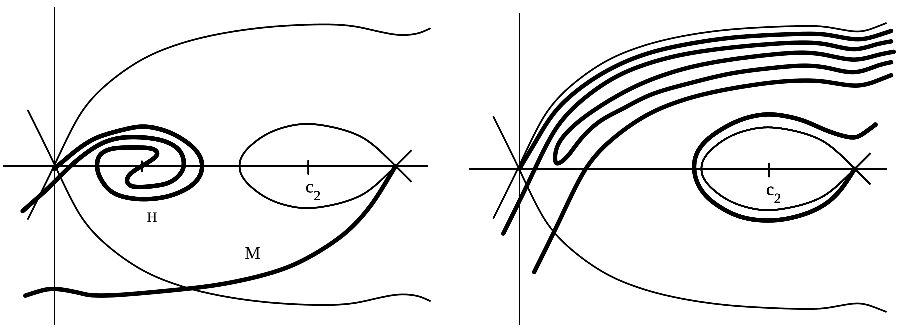

(a) Beginning (b) End

Figure 4 Undesirable evolution of L_y in the second interval

homoclinic under c_2 to the equilibrium $(1, 0)$. And now we start an inductive step: suppose that at the end of the $(i-1)$-th interval $[x_{i-2}/\epsilon, x_{i-1}/\epsilon]$, we have a number m_{i-1} of "manifolds" close to the unstable manifold of the equilibrium point that has no homoclinic orbit under c_{i-1}, and a number h_{i-1} of "hooks" that follow the homoclinic orbit under c_{i-1} (mainly from outside). Then the inductive step consists in showing that along the interval $[x_{i-1}/\epsilon, x_i/\epsilon]$, the evolution behaves as depicted in figure 5: the m_{i-1} manifolds are folded and produce m_{i-1} new hooks, and the manifolds and the hooks together produce $m_{i-1} + 2h_{i-1}$ new manifolds. So, $h_i = m_{i-1}$ and $m_i = m_{i-1} + 2h_{i-1}$.

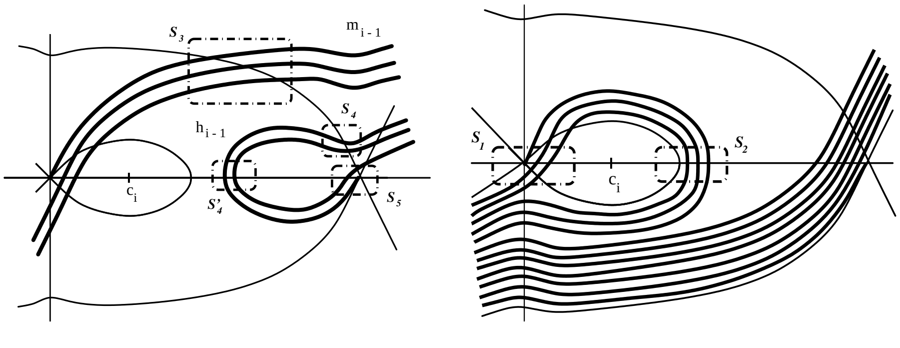

(a) Beginning (b) End

Figure 5 Evolution of L_y in the i-th interval. See sections 2 and 3 for notation.

Care must be taken at this point because "fingers" could also appear in this step from the $(i-1)$ to the i-th interval if the previous hooks do not stay mainly outside the homoclinic but start to spiral inside it, for example for ϵ very small. The condition that the c_i are alternatively close to 0 and 1 plays a fundamental role here too. See [17] for details.

k	N_k	m_k	h_k	$E_k(0)$	$E_k(1)$	$E_k(2)$	$E_k(3)$	$E_k(4)$	$E_k(5)$
0	1	1	0	1					
1	3	1	1	2	1				
2	5	3	1	3	2				
3	11	5	3	5	5	1			
4	21	11	5	8	10	3			
5	43	21	11	13	20	9	1		
6	85	43	21	21	38	22	4		
7	171	85	43	34	71	51	14	1	
8	341	171	85	55	130	111	40	5	
9	683	341	171	89	235	233	105	20	1
10	1365	683	341	144	420	474	256	65	6

Table 1 Numbers N_k of equilibria, m_k of "manifolds", h_k of "hooks", and the numbers $E_k(\mu)$ of equilibria with Morse index μ for global attractors $\mathcal{A}_k$ associated to cubic nonlinearities with $k-1$ large enough jumps, $k = 2, 3, \dots, 10$. Note that the the stable equilibria $E_k(0)$ follows the Fibonacci sequence and that $\mu_k = \dim \mathcal{A}_k = [(k+1)/2]$ for the maximal Morse index μ_k.

Suppose $i = k$ has been reached by the previous inductive steps. To find the number N_k of equilibrium solutions one then has to count the intersections of $L_{x_k/\epsilon}$ with the u-axis. Clearly $N_k = m_k + 2h_k$. From this and the previous relations, we have

$$N_k = m_k + 2h_k = m_{k-1} + 2h_{k-1} + 2m_{k-1} = N_{k-1} + 2(m_{k-2} + 2h_{k-2}) = N_{k-1} + 2N_{k-2};$$

and the statement of Theorem 2.1 follows from here. □

3 Morse indices

The Morse index of an hyperbolic equilibrium is the number of eigenvalues with strictly positive real parts of the linearised equation around this equilibrium. This section is devoted to the proof of the following result that characterises the Morse indices that appear in the set of N_k equilibria found in the previous section.

Theorem 3.1 *With the same hypotheses and notation as in Theorem 2.1, let $E_k(\mu)$ be the number of equilibria with Morse index equal to μ for integer $\mu \geq 0$ and $k \geq 2$. Then*

$$E_k(\mu) = E_{k-1}(\mu) + E_{k-2}(\mu) + E_{k-2}(\mu - 1), \tag{3.1}$$

with the initial conditions $E_0(0) = 1$, $E_0(1) = 0$, $E_1(0) = 2$, $E_1(1) = 1$, $E_0(\mu) = E_1(\mu) = 0$ for $\mu \geq 2$, and taking $E_k(\mu) = 0$ for any $k < 0$;(see table 1). All of these equilibria are hyperbolic.

Remarks 3.1

- Since $N_k = \sum_\mu E_k(\mu)$, the statement of Theorem 3.1 implies the recursion formula in Theorem 2.1.
- Since $E_k(0)$ is the number of stable equilibria, the recurrence (3.1) produces the Fibonacci sequence $3, 5, 8, 13, \dots,$ for $k = 2, 3, 4, 5, \dots.$ This fact was proved in [16]. The same sequence appears when the function $c(x)$ in (1.1) is smooth but has $k-1$ crossings with $c = 1/2$ (see [4]).

- The recurrence (3.1) also implies that the maximal Morse index is $[(k+1)/2]$, where $[\cdot]$ stands for the integer part. This fact improves one of the results of [17] where only the bound $\dim \mathcal{A}_k \leq 2k$ was given. The recurrence (3.1) also implies that the number of equilibria where this maximal Morse index is achieved is 1, when k is odd, and $1 + k/2$ when k is even. See table 1.

Proof of Theorem 3.1 The proof is based on the Sturm-Liouville result that the Morse index of a solution $(u(y), \dot{u}(y))$ of (2.1) can be computed as the net number of times that the tangent line to L_y at the point $(u(y), \dot{u}(y))$ crosses the horizontal direction in the clockwise sense along $0 \leq y \leq 1/\epsilon$ (see [16]).

A first consequence of this result is that all equilibria are hyperbolic (if ϵ is sufficiently small), since non-hyperbolicity happens only when $L_{1/\epsilon}$ is horizontal at the point $(u(1/\epsilon), \dot{u}(1/\epsilon))$. By the λ-Lemma we know that, for ϵ small enough, the intersections of $L_{1/\epsilon}$ with the u-axis align themselves with the unstable manifolds, and therefore are transverse to the u-axis. Note that the number of equilibria depend on k and not on ϵ, for ϵ small enough.

A second consequence of the Sturm-Liouville result mentioned above is that we can also define the "Morse index" of a given point of L_{y_0}, even if $y_0 < 1/\epsilon$, or if that point does not satisfy the boundary conditions. When we speak of the index of a given point y_0, we mean the net number of crossings of the tangent to L_y for $0 \leq y \leq y_0$. We are now going to trace how this index evolves along the intervals $(x_{i-1}/\epsilon, x_i/\epsilon)$, in a similar way as we did in the previous section with the evolution of the shape of L_y.

As we said in Section 2, the relevant parts of L_y for y at the ends of the intervals are either "hooks" or "manifolds", and we are interested in their intersections with $\{(u, 0) : 0 \leq u \leq 1\}$ on the u-axis. Let us write $E_i(\mu) = E_i(\mu, H) + E_i(\mu, M)$, where $E_i(\mu, H)$ stands for the number of intersections of the "hooks" of $L_{x_i/\epsilon}$ with Morse index equal to μ, and $E_i(\mu, M)$ for that of the "manifolds".

We first claim that

$$E_i(\mu, H) = E_{i-1}(\mu, M) + E_{i-1}(\mu - 1, M). \tag{3.2}$$

The intersection of the "hooks" at the end of the i-th interval can be divided into two sets of points, S_1 and S_2 (see figure 5). The first set S_1 consists of those points which have stayed in a small neighbourhood of the rest point associated to the homoclinic orbit ($(0, 0)$ in figure 5), along the whole i-th interval. These are m_{i-1} points. Because of the λ-Lemma, we see that the points in this set have not increased their Morse indices along the i-th interval, since their L_y-tangent never turned horizontal. Consequently, this first set contributes m_{i-1} intersections at the end of the interval, and with the same Morse indices as the "original" points at the end of the $(i-1)$-th. These "original" points were close to the intersections with the u-axis of the "manifolds" produced along the $(i-1)$-th interval. So, the Morse indices of S_1 are counted by $E_{i-1}(\mu, M)$.

The second set S_2 also consists of m_{i-1} points of intersection. They evolve from "original" points near the original points of S_1, but at the end of the i-th interval they are near the intersection of the homoclinic with the u-axis. By the λ-Lemma, their evolution along the i-th interval closely follows this homoclinic. So, their Morse indices have increased by 1, since there has been a single horizontal crossing of the tangent, and in the clockwise sense. In conclusion, S_2 contains the same number of points as S_1, but each Morse index has increased by 1, contributing $E_{i-1}(\mu-1, M)$ to $E_i(\mu, H)$. This proves (3.2).

Our next claim is that

$$E_i(\mu, M) = E_{i-1}(\mu). \tag{3.3}$$

Looking again at figure 5, we see that at the end of the i-th interval we can divide the intersections of the "manifolds" of $L_{x_i/\epsilon}$ with the u-axis into three new sets of points S_3, S_4 and S_5.

The set S_3 consists of m_{i-1} points of intersection, that come from "original" points near the intersection of the m_{i-1} "manifolds" with the stable manifold of the rest point that has no homoclinic orbit ($(0,1)$ in the figure). Still looking at the beginning $y = x_{i-1}/\epsilon$ of this interval, we see that each one of these points continues, along the curve $L_{x_{i-1}/\epsilon}$ and inside $0 \leq u \leq 1$, to one of the "original" points of the set S_1 considered before. But the important thing is that these two related points have the same Morse index at $y = x_{i-1}/\epsilon$.

Indeed, tangents to $L_{x_{i-1}/\epsilon}$ do not cross the horizontal axis along our continuation segment. Likewise, the corresponding continuation segment on L_0, being horizontal, does not introduce additional crossings. Therefore, the Morse indices of points related by continuation coincide. Adding up, the Morse indices of S_3 are described by the function $E_{i-1}(\mu, M)$.

Let us jump now to the last set S_5. It consists of these points which do not leave a small neighbourhood of the rest point without homoclinic orbit ($(1,0)$ in the figure) in the i-th interval. These are h_{i-1} points. Because of the λ-Lemma, we see that their Morse indices do not change along the i-th interval, since L_y avoids horizontal tangents there. Consequently, S_5 consists of h_{i-1} intersections at the end of the interval, and with the same Morse indices as their "original" points at the end of the $(i-1)$-th.

In between, there is the set S_4. Clearly it also consists of h_{i-1} points. Their "originals", at the beginning of the interval, lie near the intersections of the "hooks" produced by the $(i-1)$-th interval with the stable manifold of the rest point that has no homoclinic orbit.

As in our discussion of S_2 above, the h_{i-1} points of S_4 continue to the h_{i-1} intersection points S_4' of the "hooks", at $y = x_{i-1}/\epsilon$, to the left of the S_5 points. Unfortunately, the Morse indices in S_4 and S_4' may not coincide at $y = x_{i-1}/\epsilon$. Moreover, the Morse indices of related points in S_4' and S_5 may differ by $+1$ or -1. But we claim that, nevertheless, the Morse indices in S_4' at $y = x_{i-1}/\epsilon$ coincide with the Morse indices in S_4, at $y = x_i/\epsilon$ for points related by continuation. Indeed, the tangents to $L_{x_{i-1}/\epsilon}$ in S_4' can be deformed, artificially, to tangents of their related points in S_4, for $L_{x_i/\epsilon}$, aligning with the unstable manifold of the non-homoclinic equilibrium, without ever crossing the horizontal axis. Therefore, as in our discussion for S_2, the Morse indices of S_4' in $L_{x_{i-1}/\epsilon}$ and related points in S_4, at $L_{x_i/\epsilon}$, coincide.

The last two paragraphs show that the Morse indices of the set $S_4 \cup S_5$ are described by the function $E_{i-1}(\mu, H)$. Then, $E_i(\mu, M) = E_{i-1}(\mu, M) + E_{i-1}(\mu, H) = E_{i-1}(\mu)$, as claimed in (3.3).

Combining the claims (3.2) and (3.3) we obtain

$$\begin{aligned} E_i(\mu) &= E_i(\mu, H) + E_i(\mu, M) = E_{i-1}(\mu, M) + E_{i-1}(\mu-1, M) + E_{i-1}(\mu) = \\ &= E_{i-2}(\mu) + E_{i-2}(\mu-1) + E_{i-1}(\mu), \end{aligned} \tag{3.4}$$

as we wanted to prove.

The same arguments applied to the first and second intervals give us the initial conditions $E_1(\mu)$ and $E_2(\mu)$ of the recursion. □

4 The Global Attractor

As a consequence of the hyperbolicity of equilibria for ϵ small enough, and because of the general results of D. Henry [11] and S. Angenent [2] (see also [3], for related results), this dynamical system belongs to the important class of Morse-Smale infinite-dimensional dynamical systems, considered by W. Oliva in [13] (see also [14]).

As it is proved in [13] (see also [10]), this system is structurally stable, so although its attractor changes when making ϵ smaller and the sequence $c_1, c_2, \dots, c_k$ closer to $0, 1, 0, 1, \dots$, the global attractors will remain topologically equivalent. For this reason, one can speak about "the" limiting global attractor $\mathcal{A}_k$ corresponding to k subintervals. This section indicates some first steps towards a complete geometric analysis of the attractors $\mathcal{A}_k$.

The main tool for the description of $\mathcal{A}_k$ is the permutation associated to the N_k equilibria introduced by Fusco and Rocha [9]. This permutation $(p_k(j))$ for $j = 1, 2, \dots, N_k$ represents the different orderings between the sets $\{u_j(0) : j = 1, 2, \dots, N_k\}$ and $\{u_j(1) : j = 1, 2, \dots, N_k\}$ of boundary values of the equilibria $u_j(x)$. More precisely, if $u_1(0) < u_2(0) < \dots u_{N_k}(0)$, the permutation $p = p_k$ is defined by $u_{p(1)}(1) < u_{p(2)}(1) < \dots < u_{p(N_k)}(1)$.

It is a central property of the theory of attractors of scalar one-dimensional parabolic equations that these permutations characterise the global attractor. In fact, global attractors with the same permutation are C^0 orbit equivalent (see [7]). The permutation determines, explicitly and constructively, which equilibria are connected to which other equilibria, heteroclinically (see [6]). The arising permutations can be characterised purely combinatorially (see [8]; for explicit examples, see [5]).

To explicitly describe the arising permutations, we schematically plot the shooting curves $L_{x_k/\epsilon}$ in the $(u, \dot{u})$-plane; see figure 6. Only the schematics are relevant, since identical permutations produce equivalent attractors. Consider only the top half of figure 6, above the u-axis. It consists of four families of nested upper half circles. From left to right, the number of half circles in each family is given by the sequence $[3, 5, 1, 1] = [h_3, h_4, h_1, h_2]$, with the convention $h_1 = 1$ and h_k indicating the number of hooks from table 1.

Similarly, the families below the u-axis contain the following numbers of half circles: $[1, 3, 1, 5] = [h_1, h_3, h_2, h_4]$. Denoting h-indices, only, rather than h-values, we can represent the configuration p_4 of figure 6 above and below the u-axis, respectively, by the rows of the matrix

$$(p_4) = \begin{pmatrix} 3 & 4 & 1 & 2 \\ 1 & 3 & 2 & 4 \end{pmatrix}. \tag{4.1}$$

Note how each row itself indicates a permutation of the numbers $\{1, 2, 3, 4\}$.

Conversely, the right hand side of (4.1) determines the permutation p_4. Indeed, the schematic shooting curve is recovered, as soon as we substitute $h_j = (2^j - (-1)^j)/3$ for an entry j in the top/bottom row of (4.1). Note how the top circles omit the final crossing at $u = 1$, whereas the bottom circles omit the initial crossing at $u = 0$. Numbering crossings of the schematic shooting curve with the u-axis sequentially, as indicated in figure 6, we recover the permutation p_4^{-1}, by reading

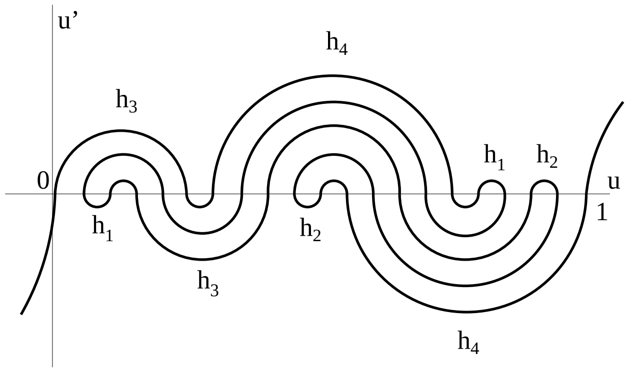

Figure 6 Schematics of shooting curve for the permutation p_4.

along the u-axis. Here we have obtained the shooting curve from its intersection at $u = 0$ to its intersection at $u = 1$. See [6] and [8] for details.

In the short hand notation of (4.1), the permutations p_k for $k = 5, 6, 7, 8$ now read as follows:

$$(p_5) = \begin{pmatrix} 5 & 3 & 4 & 1 & 2 \\ 1 & 3 & 2 & 5 & 4 \end{pmatrix}, \qquad (p_6) = \begin{pmatrix} 5 & 6 & 3 & 4 & 1 & 2 \\ 1 & 3 & 2 & 5 & 4 & 6 \end{pmatrix}, \tag{4.2}$$
$$(p_7) = \begin{pmatrix} 7 & 5 & 6 & 3 & 4 & 1 & 2 \\ 1 & 3 & 2 & 5 & 4 & 7 & 6 \end{pmatrix}, \quad (p_8) = \begin{pmatrix} 7 & 8 & 5 & 6 & 3 & 4 & 1 & 2 \\ 1 & 3 & 2 & 5 & 4 & 7 & 6 & 8 \end{pmatrix}.$$

Note the general construction principle of p_k, for arbitrary k. The bottom row is given by entries $\tau^+ = (\tau_1^+, \tau_2^+, \ldots, \tau_k^+)$, where

$$\tau_j^+ = j + (-1)^j \tag{4.3}$$

for $1 < j < k$, and $\tau_1^+ = 1$, $\tau_k^+ = k - (1 - (-1)^k)/2$. Similarly, the top row is given by entries $\tau^- = (\tau_k^-, \tau_{k-1}^-, \ldots, \tau_2^-, \tau_1^-)$, where

$$\tau_j^- = j - (-1)^j \tag{4.4}$$

for $1 \leq j < k$, and $\tau_k^- = k-(1+(-1)^k)/2$. Note the reverse order of the components in the index vector τ^-. In summary,

$$(p_k) = \begin{pmatrix} \tau^- \\ \tau^+ \end{pmatrix} \tag{4.5}$$

We do not prove the general construction principle (4.3)-(4.5) for all the permutations (p_k) here. Clearly the proof has to proceed by induction on k, keeping track of the detailed connectivity properties of the m_k "manifolds" and the h_k "hooks". These connectivity properties have been omitted, for simplicity, in [17] and in our account in Sections 2,3 of the present paper. Purely combinatorially speaking, it is even remarkable that the construction (4.3)-(4.5) gives rise to a single connected curve, thus defining a permutation p_k, for all $k \geq 2$.

With this algorithm we have obtained, for example, the following permutations:

$k = 2$: { 1, 2, 3, 4, 5 }
$k = 3$: { 1, 6, 7, 8, 5, 2, 3, 4, 9, 10, 11 }
$k = 4$: { 1, 10, 11, 12, 9, 2, 3, 8, 13, 18, 19, 20, 17, 14, 7, 4, 5, 6, 15, 16, 21 }

$k = 5$: { 1, 22, 23, 28, 17, 6, 7, 16, 29, 38, 39, 40, 37, 30, 15, 8, 5, 18, 27, 24, 21, 2, 3, 20, 25, 26, 19, 4, 9, 14, 31, 36, 41, 42, 35, 32, 13, 10, 11, 12, 33, 34, 43 }

$k = 6$: { 1, 42, 43, 52, 33, 10, 11, 32, 53, 74, 75, 76, 73, 54, 31, 12, 9, 34, 51, 44, 41, 2, 3, 40, 45, 50, 35, 8, 13, 30, 55, 72, 77, 82, 67, 60, 25, 18, 19, 24, 61, 66, 83, 84, 65, 62, 23, 20, 17, 26, 59, 68, 81, 78, 71, 56, 29, 14, 7, 36, 49, 46, 39, 4, 5, 38, 47, 48, 37, 6, 15, 28, 57, 70, 79, 80, 69, 58, 27, 16, 21, 22, 63, 64, 85 }

With these permutations at hand it is possible to reconstruct all connections inside $\mathcal{A}_k$, see [5] and [6].

The geometry of the first five attractors, which are the ones that can be embedded on a three-dimensional space is depicted in figures 7 and 8 (the cases $k = 0$ and $k = 1$ are artificial) .

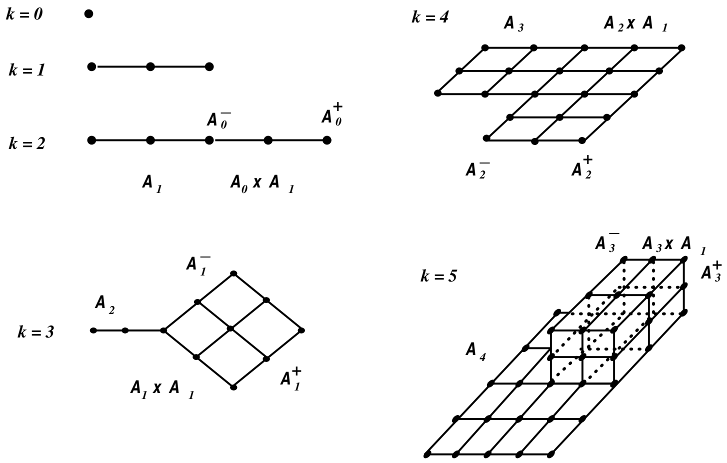

Figure 7 Geometry of the attractors $\mathcal{A}_{k+1}$ for $k+1 = 0, 1, \ldots, 5$.

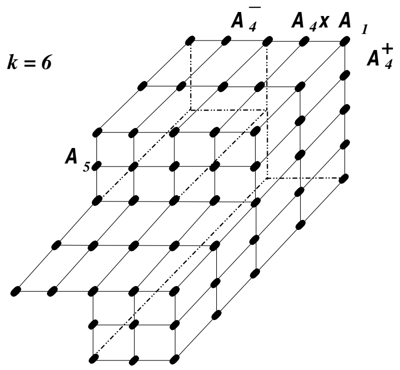

Figure 8 Geometry of the attractor $\mathcal{A}_6$. See conjecture for recursive construction.

These figures suggest the following conjecture for a geometric recursion of the global attractors $\mathcal{A}_k$, in the limit of small positive ϵ.

Conjecture 4.1 *Let $\mathcal{A}_0$ denote a single point, and $\mathcal{A}_1 \subset \mathbb{R}$ denote the global attractor of the cubic ODE $\dot{v} = v(1-v^2)$. Then*

$$\mathcal{A}_{k+1} \cong (\mathcal{A}_k \hookleftarrow \mathcal{A}_{k-1} \times \mathcal{A}_1 \to \mathcal{A}_{k-1}) \tag{4.6}$$

for all $k \geq 1$.

We explain the notation in (4.6). The term $\mathcal{A}_{k-1} \times \mathcal{A}_1$ indicates direct product flow on the Cartesian product. In other words, $\mathcal{A}_{k-1} \times \mathcal{A}_1$ contains three copies of $\mathcal{A}_{k-1}$. Two of these copies, $\mathcal{A}_{k-1}^{\pm}$, corresponding to $v = \pm 1$ in $\mathcal{A}_1$, are normally attracting. The third copy, $\mathcal{A}_{k-1}^0$, which corresponds to $v = 0$, provides a normally one-dimensionally unstable suspension of $\mathcal{A}_{k-1}$. Heteroclinic orbits within $\mathcal{A}_{k-1}$ are lifted to three copies within $\mathcal{A}_{k-1}^0$ and $\mathcal{A}_{k-1}^{\pm}$, respectively. For example, $\mathcal{A}_1 = \mathcal{A}_0 \times \mathcal{A}_1$.

The symbol $\cong$ indicates C^0 orbit equivalence. The arrows $\hookleftarrow$ and $\to$ indicate certain substitutions for the copies $\mathcal{A}_{k-1}^{\pm}$ of $\mathcal{A}_{k-1}$ in the direct product flow of $\mathcal{A}_{k-1} \times \mathcal{A}_1$. The arrow $\to \mathcal{A}_{k-1}$ indicates that, indeed, $\mathcal{A}_{k-1}^{+}$ is replaced by just a copy of $\mathcal{A}_{k-1}$, as was described above. The embedding arrow $\hookleftarrow$, in contrast, indicates that $\mathcal{A}_{k-1}^{-}$ above has to be replaced by a copy of $\mathcal{A}_k$ rather than just by a copy of $\mathcal{A}_{k-1}$. This is possible, because we can identify a unique copy of $\mathcal{A}_{k-1}$ in $\mathcal{A}_k$: we take the copy of $\mathcal{A}_{k-1}$which appeared in (4.6) as the leftmost entry in the previous construction of $\mathcal{A}_k$, according to

$$\mathcal{A}_k \cong (\mathcal{A}_{k-1} \hookleftarrow \mathcal{A}_{k-2} \times \mathcal{A}_1 \to \mathcal{A}_{k-2}). \tag{4.7}$$

For $k = 1$, we take $\mathcal{A}_0 \subset \mathcal{A}_1$ to represent the equilibrium $v = -1$.

The conjecture is not limited to just indicating the graph of all (one-dimensional) heteroclinic orbits. It was already observed in [6] that transitivity in Morse-Smale systems, as established by W. Oliva in [10] and [13] together with a "cascading principle" makes it sufficient to know all the heteroclinic orbits between equilibria of Morse index differing by 1. Indeed, all other heteroclinic connections follow (cascading) sequences of such (unique) one-dimensional heteroclinic orbits. The conjecture contains a geometric statement: the C^0 orbit equivalence of the global attractors $\mathcal{A}_k$ to the models described above. Strictly speaking, this geometric part of the conjecture has not even been established for the attractor $\mathcal{A}_5$, depicted in figure 7.

Observe that the statement of this conjecture obviously includes Theorems 2.1 and 3.1 of the present paper.

References

[1] Nicholas D. Alikakos, Peter W. Bates, and Giorgio Fusco. Solutions to the nonautonomous bistable equation with specified morse index. Part I: Existence. *Transactions of the American Mathematical Society*, 340(2):641–654, 1993.

[2] Sigurd B. Angenent. The morse-smale property for a semi-linear parabolic equation. *Journal of Differential Equations*, 62(3):427–442, 1986.

[3] Sigurd B. Angenent. The zero set of a solution of a parabolic equation. *J. Reine Angew. Math.*, 390:79–96, 1988.

[4] Sigurd B. Angenent, John Mallet-Paret, and Lambertus A. Peletier. Stable transition layers in a semilinear boundary value problem. *Journal of Differential Equations*, 67:212–242, 1987.

[5] Bernold Fiedler. Global attrators of one-dimensional parabolic equations: sixteen examples. *Tatra Mountains Math. Publ.*, 4:67–92, 1996.

[6] Bernold Fiedler and Carlos Rocha. Heteroclinic orbits of semilinear parabolic equations. *Journal of Differential Equations*, 125(1):239–281, 1996.

[7] Bernold Fiedler and Carlos Rocha. Orbit equivalence of global attractors of semilinear parabolic differential equations. *Transactions of the American Mathematical Society*, 352(1):257–284, 1999.

[8] Bernold Fiedler and Carlos Rocha. Realization of meander permutations by boundary value problems. *Journal of Differential Equations*, 156(2):282–308, 1999.

[9] Giorgio Fusco and Carlos Rocha. A permutation related to the dynamics of a scalar parabolic pde. *Journal of Differential Equations*, 91(1):111–137, 1991.

[10] Jack K. Hale, Luis T. Magalhães, and Waldyr M. Oliva. *An Introduction to Infinite Dimensional Dynamical Systems—Geometric Theory*, volume 47 of *Appl. Math. Sci.* Springer-Verlag, New York, 1984.

[11] Daniel Henry. Some infinite-dimensional morse-smale systems defined by parabolic partial differential equations. *Journal of Differential Equations*, 59(2):165–205, 1985.

[12] Henry L. Kurland. Monotone and oscillatory equilibrium solutions of a problem arising in population genetics. In *Nonlinear Partial Differential Equations*, volume 17 of *Contemporary Mathematics*, pages 323–342. American Mathematical Society, 1983.

[13] Waldyr M. Oliva. *Stability of Morse-Smale Maps.* Rel. Tec., IME-USP, São Paulo, MAP 0301, (1983).

[14] Waldyr M. Oliva. Morse-Smale semiflows. Openness and A-stability. Preprint, 2000.

[15] Jacob Palis, Jr. and Welington de Melo. *Geometric Theory of Dynamical Systems.* Springer Verlag, 1982.

[16] Carlos Rocha. Examples of attractors in scalar reaction-diffusion equations. *Journal of Differential Equations*, 73(1):178–195, 1988.

[17] Domingo Salazar and Joan Solà-Morales. On the number and indices of equilibria in a space-dependent bistable parabolic equation. *Nonlinearity*, 14:121–132, 2001.